Electromagnetic Scattering Computation Using a Hybrid Surface and Volume Integral Equation Formulation

Chong Luo and Cai-Cheng Lu

Electrical Computer Engineering Department, University of Kentucky
Lexington, Kentucky, USA

Abstract **–** This paper presents a hybrid integral equation formulation for computation of electromagnetic scattering by composite conducting and dielectric materials. In the hybrid formulation, multiple material regions in a scatterer are classified into two categories, one is the surface integral equation (SIE) region, and the other is the volume integral equation (VIE) region. For the SIE region, the boundary conditions for tangential E-field and tangential H-field are applied to formulate the surface integral equation for the equivalent surface currents. For the VIE region, the equivalent principle is applied to formulate the volume integral equation for the induced volume currents. The hybrid formulation takes the advantageous of both the SIE and VIE. The integral equations are cast into a set of linear equations using the method of moments. For regions that are electrically large, the multilevel fast multipole algorithm is applied to accelerate the matrix-vector multiplication needed by iterative solvers. Numerical results are provided to verify the accuracy and the application of the program developed from the hybrid formulation.

Key words **–** Scattering/RCS, method of moments, hybrid methods, and boundary integral equations.

I. INTRODUCTION

The integral equation approach has been used to model electromagnetic scattering by perfectly electrical conducting objects as well as dielectric materials. When this approach is used to solve an electromagnetic wave scattering problem involving piece-wise homogeneous electric and magnetic materials, there are two frequently used formulations: the surface integral equation (SIE) formulation [1-10] and the volume integral equation (VIE) formulation [11-16]. In SIE formulation, unknown equivalent electric current and magnetic current are assigned on the material surfaces, as well as the perfectly electrical conducting (PEC) surfaces. The boundary conditions of tangential E-field and tangential H-field across material surfaces are applied to formulate the SIE for the equivalent currents. In the VIE formulation, equivalent electric and magnetic volume currents are assigned to the volumes occupied by the materials. The field equivalence principle[1] is applied to formulate the volume integral equations for the volume currents. Both the SIE and VIE formulations have their own advantageous depending on the problem to be solved and on the way the discretized linear equation is solved. In general, the SIE formulation leads to less number of unknowns for electrically large material volume regions compared to that of the VIE formulation. If a problem consists of materials of electrically thin cylinders and thin slabs, it is expected that both SIE and VIE formulation will have comparable numbers of unknowns. However, If iterative solvers are used to solve the discretized linear equations, the VIE formulation will have higher converge rate (or need less number of iterations) because it is of the second kind [18]. Based on the above comparisons, we propose a hybrid SIE and VIE formulation. In this way, the material volumes are classified into two groups. The electrically large and bulk material volumes belong to one group for which the SIE formulation is applied (the SIE also applied to the perfectly electric conducting surfaces). The other group consists of material volumes that are electrically thin or small (such as the thin slabs and cylinders) for which the VIE formulation is applied. We call this approach the "SIE+VIE" approach. The purpose is to take the advantageous of the "SIE ONLY" and "VIE ONLY" approaches, and avoid the drawbacks of the two. It is difficult to draw a line on the use of VIE and SIE for a given material region. As a general guideline, large, thick, and homogeneous material regions are modeled by SIE, and small, thin and inhomogeneous material regions are modeled by VIE. In the following, we will present the hybrid formulation of the "SIE+VIE" approach, followed by numerical examples to verify the implementation. For a composite scatterer with piece-wise dielectric material, we can solve the problem using any one of the three approaches, i.e., the hybrid "SIE+VIE", the "SIE ONLY", and the "VIE ONLY". It must be emphasized that in all three approaches, SIE is applied to PEC surfaces. The distinction lies in the treatment of material. In the "SIE ONLY" approach, SIE is applied to all material surfaces (hence it can only deal with piece-wise homogeneous scatterers); in the "VIE ONLY" approach, VIE is applied to all material volumes; and in the hybrid "SIE+VIE" approach, part of the material region is modeled by SIE and the rest are modeled by VIE. The formulation is in frequency domain, and the time factor of $\exp\{-i\omega t\}$ is implied and suppressed in all the equations.

[1] A rigorous derivation of VIE can be found in a recent paper by M. Sencer *et al* in [17].

II. FORMULATION

A general scatterer usually consists of PEC surfaces and electric/magnetic materials regions, as shown in Fig. 1. In the "SIE+VIE" formulation, the volume integral equation is constructed for the small or inhomogeneous material regions, and the surface integral equation is constructed for PEC surfaces and the surfaces of large homogeneous material regions. Although pure SIE formulation (the "SIE ONLY") could be applied to all the piece-wise material regions, it can be inefficient if there are small and thin material volumes to which the VIE formulation is more efficient and will lead to a better conditioned system equation [18].

A. Integral Equations

To simplify the notation, we first define two operators, $\bar{\bar{L}}$ and $\bar{\bar{K}}$, such that,

$$\bar{\bar{L}}_j \cdot \vec{J} = \int_\Omega (\bar{\bar{I}} + \frac{1}{k_j^2}\nabla\nabla) G(\vec{r},\vec{r}',k_j)\cdot \vec{J}(\vec{r}')d\Omega, \qquad (1)$$

$$\bar{\bar{K}}_j \cdot \vec{M} = \nabla\times\int_\Omega G(\vec{r},\vec{r}',k_j)\vec{M}(\vec{r}')d\Omega, \qquad (2)$$

where the integral domain Ω could be either a surface or a volume, $G(\vec{r},\vec{r}',k_j)=\exp(ik_j|\vec{r}-\vec{r}'|)\ /(4\pi|\vec{r}-\vec{r}'|)$ is the 3-D scalar Green's function for unbounded homogeneous material space with constant wavenumber $k_j=\omega\sqrt{\varepsilon_j\mu_j}$, and $\bar{\bar{I}}$ is the identity dyad.

Before explaining the general scattering configurations, we first consider a few simple cases. The focus is on introducing the domains for a scattering configuration. The details of the equivalence problem and integral equation formulation will be discussed afterwards. To illustrate the configuration in general, we first consider several simple cases. (1) If a PEC sphere is in a free-space, then the configuration consists of one domain (the whole space) with one PEC body embedded within it. The domain boundary is S_∞ (a spherical surface of infinite radius). This surface S_∞ is implied for all infinite regions, and is ignored in all cases since no integral equation is formulated on it. In this case, one SIE is constructed on the PEC surface for the induced electric current. (2) If a dielectric body is in free-space and it is to be modeled by VIE, then the configuration has one domain, and the dielectric body is said to be embedded within this domain. One VIE is formulated for the dielectric volume (assuming non-magnetic case). (3) If a homogeneous material sphere resides in a free-space, and SIE is used to model the scattering of the material, then the configuration consists of two domains that are separated by a spherical surface (the interior domain R_1 and the exterior domain R_2). The spherical surface is named S_1 for R_1, and S_2 for R_2. Two SIEs are formulated on S_1, and two SIEs are formulated for S_2 (equation redundancy will be considered later). (4) Now we consider a two-layer dielectric sphere in free-space. There are two concentric spherical surfaces with radii a_1 and a_2 ($a_1<a_2$), respectively. If the hybrid "SIE+VIE" is applied to this problem, there are at least two possibilities. In one case, the spherical core is considered as embedded within a dielectric sphere of radius a_2, and it is modeled by VIE. In this case, the overall configuration has two domains, one (R_1) is interior to the larger sphere ($r\le a_2$, including the core region), and the other (R_2) is the exterior one ($r\ge a_2$). The two domains share the same spherical surface of radius a_2. This surface is named S_1 for R_1, and S_2 for R_2. Equivalent problem for R_2 leads to two SIEs on S_2, and the equivalent problem for R_1 leads to two SIEs on S_1, and one VIE for the embedded core volume. In the other case, the scatterer is considered as a thin layer of coating on a homogeneous sphere of radius a_1. The coating is modeled by VIE. In this case, the overall configuration has two domains as well, domain R_1 is the spherical space of $r\le a_1$, and domain R_2 is the rest of the whole space ($r\ge a_1$). The two domains share the same spherical surface $r=a_1$. This surface is named S_1 for R_1, and S_2 for R_2. The equivalent problem for R_1 leads to two SIEs on S_1, and the equivalent problem for R_2 leads to two SIEs on S_2, and one VIE for the embedded dielectric shell coating. Of the two cases, one is more efficient sometimes than the other depending on the relative sizes of each part. For example, case one will be more efficient if the dielectric core has radius much less than a wavelength, and case two is more efficient if the shell thickness (a_2-a_1) is much smaller than a wavelength.

With the above discussions, we consider the sketch of a general scatterer shown in Fig. 1. It consists of PEC bodies (denoted by $\sigma=\infty$), and a number of piece-wise homogeneous material domains $R_1,R_2,\cdots,R_n$ (with complex material parameters of ε_i,μ_i, $i=1,2,\cdots,n$), and a number of un-named material regions (shown by the dot-shaded regions in the figure) embedded within the existing domains. These embedded regions are not numbered and will be modeled by VIE. For instance, the region marked by $\vec{J}_{V2}$ is embedded within R_2. Let S_{ij} be the surface shared by domain R_i and R_j, and S_{pj} be the conducting surface that is exposed to domain R_j. In addition, we define S_i to be the boundary of domain R_i, it may be a union of several open surfaces. For example, S_3 is the boundary of R_3 and it is the union of $S_{31},S_{32},S_{34},$ and S_{3n} (highlighted by thick solid lines in Fig. 1), i.e., $S_3=\cup\{S_{13},S_{23},S_{34},S_{3n}\}$. If there are PEC regions embedded within R_3, then the conducting surfaces shall also be part of S_3.

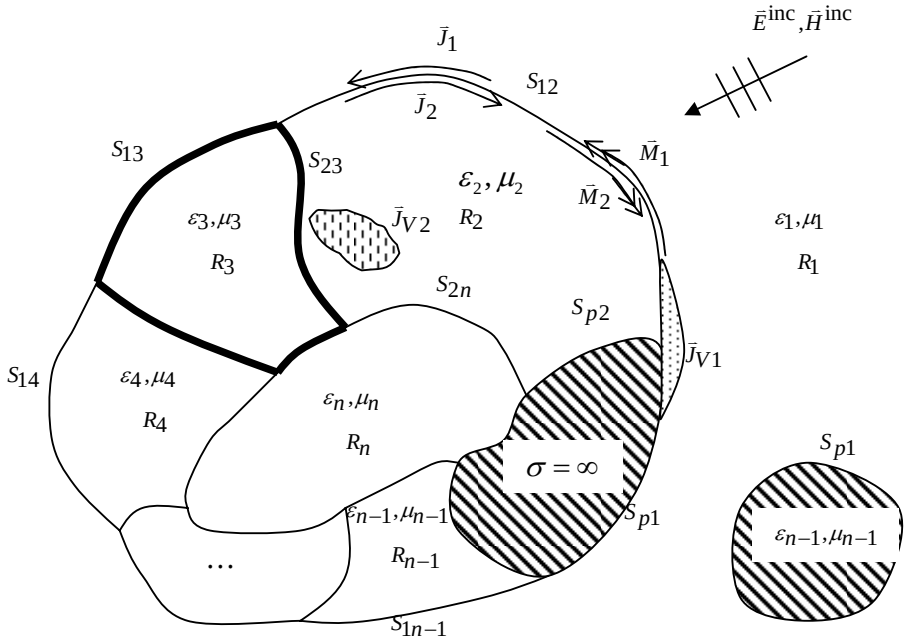

Fig. 1. A sketch of a general scatterer that is made of PEC bodies as well as multiple piece-wise homogeneous dielectric materials within which inhomogeneous materials may be embedded.

The equivalent problems for the domains are formed independently from each other. For example, the equivalent problem for R_1 is shown in Fig. 2. It is obtained by removing all materials exterior to boundary S_1 (highlighted by thick dotted line), all PEC bodies within S_1, and then filling the left over space with the same material as that of region R_1. The total electric field and magnetic field are set to zeros for the region exterior to S_1, and equivalent electric current $\bar{J}_1$ and magnetic current $\bar{M}_1$ are introduced on surface S_1.

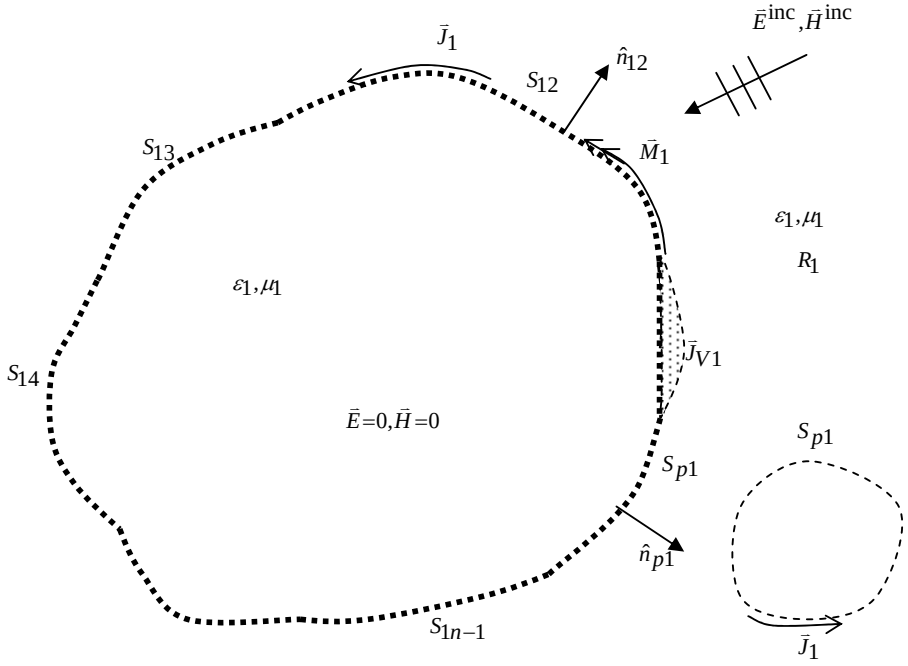

Fig. 2. Equivalent problem for region R_1.

Meanwhile, the material body embedded within R_1 is removed and the equivalent volume current $\bar{J}_{V1}$ is introduced for that volume. This is repeated for all such embedded material bodies (for simplicity of derivation, we will not consider embedded magnetic material in this paper. If embedded magnetic material presents, then additional volume integral equation for equivalent magnetic volume current shall be formulated in the same way).

Applying the boundary conditions of continuous tangential field components for the portion of S_1 that is originally the interface of materials, i.e., $S_{1i}\,(i=1,2,3,\ldots n)$ in R_1, electric field integral equation (EFIE) and magnetic field integral equation (MFIE) can be established as,

$$\hat{n}_{1i}\times\left(\vec{E}_1^{\,\mathrm{sca}}+\vec{E}_1^{\,\mathrm{inc}}\right)=-\vec{M}_1\,, \tag{3}$$

$$\hat{n}_{1i}\times\left(\vec{H}_1^{\,\mathrm{sca}}+\vec{H}_1^{\,\mathrm{inc}}\right)=\bar{J}_1\,, \tag{4}$$

where

$$\vec{E}_1^{\,\mathrm{sca}}=ik_1\eta_1\bar{\bar{L}}_1\cdot\bar{J}_1-\bar{\bar{K}}_1\cdot\vec{M}_1+ik_1\eta_1\bar{\bar{L}}_1\cdot\bar{J}_{V1}\,,$$
$$\vec{H}_1^{\,\mathrm{sca}}=\bar{\bar{K}}_1\cdot\bar{J}_1+ik_1\eta_1^{-1}\bar{\bar{L}}_1\cdot\vec{M}_1+\bar{\bar{K}}_1\cdot\bar{J}_{V1}\,.$$

The unit vector $\hat{n}_{1i}$ in equations (3) and (4) is the normal direction on surface S_{1i} that points in to R_1, and $\vec{E}_1^{\,\mathrm{inc}}$ is the primary field generated by sources in R_1 ($\vec{E}_1^{\,\mathrm{inc}}$ is calculated assuming that the sources in R_1 radiate into an unbounded homogeneous space of k_1). The EFIE on the PEC surface S_{p1}, is established using the vanishing tangential field boundary condition as

$$\hat{n}_{p1}\times\left(\vec{E}_1^{\,\mathrm{sca}}+\vec{E}_1^{\,\mathrm{inc}}\right)=0\,, \tag{5}$$

where $\hat{n}_{p1}$ is the normal direction of S_{p1} directed outward of the conductor.

In the volume material portion, the total electric field is the superposition of the incident and the scattered field. Based on this fact, VIE in domain R_1 is constructed as

$$\vec{E}_1^{\,\mathrm{sca}}-\vec{E}_1^{\,\mathrm{tot}}=-\vec{E}_1^{\,\mathrm{inc}}\,. \tag{6}$$

The volume electric current $\bar{J}_{V1}$ in equation (6) is related to the total electric field intensity by $\bar{J}_{V1}=i\omega(\varepsilon-\varepsilon_1)\vec{E}_1^{\,\mathrm{tot}}$, with ε being the position dependent permittivity for the material body embedded in V_1, and $\vec{E}_1^{\,\mathrm{tot}}=\vec{E}_1^{\,\mathrm{sca}}+\vec{E}_1^{\,\mathrm{inc}}$ is the total electric field within V_1. Thus, we have established a set of four integral equations, (3) to (6), for domain R_1. Moreover, if the conducting surface S_{p1} is a closed surface, the MFIE (magnetic field integral equation) or CFIE (combined field integral equation) can be used to replace equation (5). It should be pointed out that equation (5) will not appear for R_1 if S_1 does not contain any PEC surfaces, and equation (6) will not appear for R_1 if there are no embedded dielectric volumes in R_1.

Similarly, the equivalent problem of R_2 can be established as shown in Fig. 3.

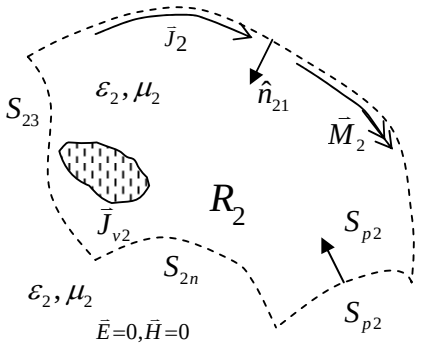

Fig. 3. Equivalent problem of domain R_2 for which the whole space (both interior and exterior to S_2) is filled with the same material of ε_2,μ_2.

The surface integral equations on the material surface S_2 (or $\cup S_{2i}$) are also based on the boundary conditions of tangential E and H fields, i.e.,

$$\hat{n}_{2i}\times\left(\vec{E}_2^{\,\mathrm{sca}}+\vec{E}_2^{\,\mathrm{inc}}\right)=-\vec{M}_2\,, \tag{7}$$

$$\hat{n}_{2i}\times\left(\vec{H}_2^{\,\mathrm{sca}}+\vec{H}_2^{\,\mathrm{inc}}\right)=\bar{J}_2\,, \tag{8}$$

where

$$\vec{E}_2^{\,\mathrm{sca}}=ik_2\eta_2\bar{\bar{L}}_2\cdot\bar{J}_2-\bar{\bar{K}}_2\cdot\vec{M}_2+ik_2\eta_2\bar{\bar{L}}_2\cdot\bar{J}_{V2}\,,$$
$$\vec{H}_2^{\,\mathrm{sca}}=\bar{\bar{K}}_2\cdot\bar{J}_2+ik_2\eta_2^{-1}\bar{\bar{L}}_2\cdot\vec{M}_2+\bar{\bar{K}}_2\cdot\bar{J}_{V2}\,.$$

The volume integral equation for V_2 is constructed in the same way as in equation (5). It is given by

$$\vec{E}_2^{\,\mathrm{sca}}-\vec{E}_2^{\,\mathrm{tot}}=-\vec{E}_2^{\,\mathrm{inc}}\,. \tag{9}$$

As stated previously, the vector $\vec{E}_2^{\,\mathrm{tot}}$ is related to the volume current by $\bar{J}_{V2}=i\omega(\varepsilon-\varepsilon_2)\vec{E}_2^{\,\mathrm{tot}}$.

Now we have established a set of three integral equations for domain R_2 (if there are PEC bodies within R_2, there would be one more surface integral equation for the PEC surfaces). This process can be repeated for all the remaining domains, $R_3,R_4,\cdots,R_n$. It is expected that for each domain, a set of two to four integral equations are established depending on whether PEC surfaces and embedded dielectric material exist in that domain. We have an overall of n sets of integral equations. It is observed that there are redundant unknown vectors assigned in the integral

equations. The redundancy is removed by using the fact that $\vec{J}$ and $\vec{M}$ on the two sides of any material interface are equal in magnitude and opposite in direction. For example, on interface S_{12} shared by domains R_1 and R_2, we have,

$$\hat{n}_{12} = -\hat{n}_{21},\ \vec{J}_1 = -\vec{J}_2 \text{ and } \vec{M}_1 = -\vec{M}_2 . \qquad (10)$$

In this way, we have only two unknown functions on each interface that is shared by two material domains. By utilizing the above relationships for $\vec{r} \in S_{12}$, we can add equations (7) to (3), and equations (8) to (4), to reduce the number of equations from four to two (this approach was proposed in a paper by Wu and Tsai [4] based on the earlier work of Poggio, Miller, Chang, Harrington, Wu, and Tsai, and hence the formulation is called PMCHWT). In this paper, the SIE applied to dielectric material surfaces refers to this PMCHWT formulation. It shall be noted that there are other ways to combine the integral equations leading to different SIE formulations.

B. Discretization of the Integral Equations

When all the integral equations are established, we apply the method of moments (MoM) to descritize the integral equations into a set of N linear algebra equations. Once again, the integral equations formulated for each domain are discretized before they are combined with those of the other domains to remove redundancy. To this end, the surfaces are modeled by a set of electrically small and nearly flat quadrangles, and the volumes are modeled by a set of electrically small hexahedron elements whose six faces are also nearly flat quadrangles. Basic requirements on the mesh are,

(a) All quadrangles are well connected (two quadrangles can share no more than two nodes, and if they share two nodes, then they must share an edge).

(b) All hexahedrons are well connected (two hexahedrons can share no more than four nodes, and if they share four nodes, then they must share a common face).

(c) All quadrangles and hexahedrons are also well connected. If the number of shared nodes between a quadrangle and a hexahedron is n, then (a) n must be 0,1,2,4 only; (b) if n = 2, they must share a common edge; (c) if n = 4, the quadrangle must overlap with a face of the hexahedron.

(d) All mesh nodes must be vertices of quadrangles and/or hexahedrons (no mesh nodes are allowed inside a mesh element or interior to the boundary of it.

Then surface roof-top basis functions are used to expand the surface vectors ($\vec{J}$ and $\vec{M}$), and the volume roof-top basis functions are used to expand the volume vector $\vec{J}_V$. A volume roof-top basis function is defined on two neighboring hexahedrons that share a common face (if a face of a hexahedron is not shared, a volume basis function is also assigned to this face [12], and this basis function is called a half basis). A surface roof-top basis function is defined on two or more neighbor quadrangles that share a common edge. If an edge is shared by more than two quadrangles, it is a junction edge [5] (no half basis is defined for surface mesh). There are several types of junctions that must be treated differently. Here we consider two simple types of junctions: (1) all quadrangles that share a common edge are material interfaces. In this case, one basis function is assigned to the junction; (2) Multiple material quadrangles are connected to an edge shared by two PEC quadrangles that on a PEC body of non-zero thickness. In this case, one basis function is assigned to the junction. Both the surface and volume basis functions can be written in the following form [18],

$$\vec{f}_i^{\,\Omega}(\vec{r}) = \frac{\pm 1}{\sqrt{g}} u \frac{\partial \vec{r}}{\partial u}, \quad \vec{r} \in \Omega, \quad \Omega = S_i \text{ or } V_i , \qquad (11)$$

where S_i (or V_i) is a surface (or volume) mesh element, $\sqrt{g}$ is the Jacobian of the transformation that maps a mesh element in (x,y,z) coordinate system into a unit element in the (u,v,w) coordinate system. In the (u,v,w) space, a unit quadrangle is a square defined by $0 \le u \le 1,$, $0 \le v \le 1,$ and $w = 0$, and a unit hexahedron is a cube defined by $0 \le u \le 1,$ $0 \le v \le 1,$ and $0 \le w \le 1$. More details on the discretization can be found in [12,18]. After discretization, we get a set of n matrix equations, one set for each domain, as follows,

$$\bar{\bar{A}}_i \cdot \bar{x}_i = \bar{b}_i , \quad i = 1,2,\cdots,n , \qquad (12)$$

where, $\bar{\bar{A}}_i$ is the impedance matrix of size $N_i \times N_i$ for the integral operators, $\bar{x}_i$ is a vector of length N_i whose components are the expansion coefficients for the unknown vectors, and $\bar{b}_i$ is the excitation vector of length N_i that is determined by the sources, all associated with domain R_i (if R_i does not contain any source, then $\bar{b}_i = 0$). If the matrix equations are to be solved by a direct solver, then the matrices $\bar{\bar{A}}_i$, $i = 1,2,\cdots,n$, must be combined to form the system matrix $\bar{\bar{A}}$ of dimension $N \times N$ using the relationships in equation (10), where N is the total number of independent unknowns. It shall be noted that N is not a simple summation of N_i , for $i = 1,2,\cdots,n$. In general, $N \le \sum_i N_i$. If fast solvers are utilized to speed-up the solution, the linear equations are not combined until the matrix-vector product for each domain, $\bar{\bar{A}}_i \cdot \bar{x}_i$, is completed. This is discussed in the next sub-section.

C. Solution using Multilevel Fast Multipole Algorithm

For many realistic scattering problems, the electrical size of certain or all domains can be very large, and direct solvers may not be feasible. In this case, fast iterative solvers are needed to reduce the computational complexity as well as memory requirement. In general, different fast solvers can be applied to different domains depending on the size and the shape of the domains. In this paper, we apply the multilevel fast multipole algorithm (MLFMA) for all domains that is electrically large. MLFMA has been discussed in detail in many publications such as [19, 20], we focus on the implementation for multi-region problems here. To this end, we first identify the regions for which fast solvers will be applied. This is done by calculating the maximum electrical dimension D_i / λ_i of each domain R_i. If $D_i / \lambda_i \geq 1.0$, then fast solver is applied for this region (this criteria depends on the implementation). For the rest domains that do not need the fast solvers, as well as the near-neighbor interaction of any fast-solver domain, the matrices are combined and stored into one sparse matrix $\bar{\bar{A}}_0$ and direct method is applied to perform $\bar{\bar{A}}_0 \cdot \bar{x}$. For a domain R_i that MLFMA is applied, then $\bar{\bar{A}}_i \cdot \bar{x}_i$ will be performed in the same way as in a single domain problem, and $N_i \log N_i$ floating point operations are needed. The overall operation count per iteration is then made of two parts, one part is $T_1 = O(N_0)$ (N_0 is the number of non-zero entries in $\bar{\bar{A}}_0$), and the other part is

$$T_2 = \sum_i C_i N_i \log N_i \tag{13}$$

where i runs over all the domains to which MLFMA are applied, and C_i is a constant determined by the MLFMA implementation.

As a summary, the procedure to perform a matrix-vector product $\bar{y} = \bar{\bar{A}} \cdot \bar{x}$ include the following steps:

(a) For a given trial vector $\bar{x}$ in any iteration, formulate $\bar{x}_i$ (using (10) for domain R_i to which MLFMA is applied).

(b) Perform $\bar{y}_i = \bar{\bar{A}}_i \cdot \bar{x}_i$ using MLFMA in R_i.

(c) Repeat steps (a) and (b) for all domains in which MLFMA are applied.

(d) Formation of $\bar{y}' = \bigcup_i \{\bar{y}_i\}$. The union operation uses the rule of equation (10).

(e) $\bar{y} = \bar{\bar{A}}_0 \cdot \bar{x} + \bar{y}'$.

Using the above processes, a test program is written for the case of $n=2$ and numerical results are generated and shown in the next section to validate the method and to demonstrate the applications.

III. NUMERICAL RESULTS

This section provides numerical examples using the program developed for the "SIE+VIE" method. The examples are designed to consider several typical application configurations that include,

(1) Spherical structure that can use Mie series to verify the results (example 1).

(2) A large homogeneous material with small and thin materials embedding (examples 1 and 3).

(3) Small or thin materials are outside a large homogeneous material region (example 4).

(4) Structures with flat faces and edges (example 3).

(5) Structures with curved faces and edges (examples 1, 2, and 4).

(6) Structures with bulk material for which VIE is inefficient (example 2).

For example 1, we use the exact solution as a comparison. For the rest of the examples, two approaches, "SIE+VIE", and "VIE ONLY", are applied to solve the problems and results are compared to each other. In both approaches, CFIE is used for the closed PEC surfaces. The difference of the two approaches lies in the treatment of the material regions. In the "SIE+VIE" approach that is introduced in this paper, part of the material regions (normally small or thin regions) are modeled by VIE, and the large and thick material regions are modeled by SIE. The results from this approach are labeled as "SIE+VIE" in the figures. It should be noted that the VIE modeled material can be inside (embedded in) or outside the SIE material surfaces. The second approach uses VIE to model all materials, and the results are labeled as "VIE ONLY" (The terms of "VIE ONLY", "VIE+SIE", and "SIE ONLY", are introduced to mark the results and they refer to the ways materials are handled. In all cases, the surface integral equation is applied to PEC surfaces, including "VIE ONLY" approach). The "VIE ONLY" modeling is used as a way of validating the numerical results of "SIE+VIE" approach. Hence the examples are designed so that both approaches can be applied. Because of this, the run time parameters are provided for reference only. They shall not be used to determine which approach is more efficient for certain examples. All calculations are performed on a HP Superdome computer with 1.5 GHz processor and 2GB of memory.

The first example is a layered spherical structure. It consists of a PEC core (radius 0.45 m) covered by two layers of dielectric materials. The inner layer has thickness 0.05 m with relative permittivity $\varepsilon_{r2} = 4.0$; The outer layer has thickness 0.3 m with $\varepsilon_{r1} = 2.0 + 0.1i$. In the "SIE+VIE" approach, the inner layer of the coating is considered as embedded within a shell of inner radius 0.45 m, and outer radius of 0.8 m. The PEC surface and the outermost spherical surface are modeled by a total of 5,592 quadrangles (1,536 for PEC surface, and 4,056 for the outermost spherical surface). The embedded material shell of thickness 0.05

m is modeled by 1,536 hexahedron element (VIE mesh). The total number of independent unknowns for the hybrid formulation of "SIE+VIE" is N = 25,440, and the memory used is M = 469 MB. Computed bi-static RCSs for $\theta^i=0^\circ$ incidence at 300MHz are plotted in Fig. 4. The exact solutions from Mie series are also plotted for comparison. If we use the RMS error defined as

$$\text{RMS ERROR} = \sqrt{\frac{1}{n}\sum_{i=0}^{n}(\sigma_i-\sigma_i^{\text{ref}})^2}$$

to measure the difference of our solution σ_i and reference solution σ_i^{ref}, for i=1,2,...,n=181 (angles), the errors are 0.5dB for V-V, and 0.23dB for H-H polarizations, respectively.

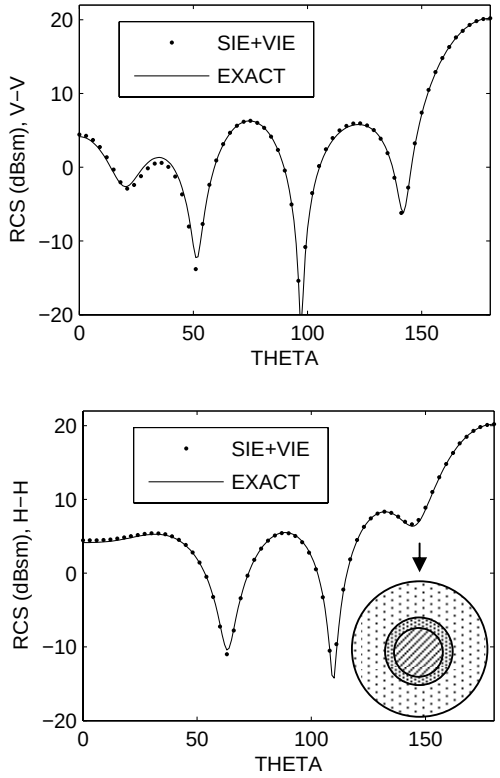

Fig. 4. Bi-static RCSs of a layered spherical scatterer for two polarizations: V-V (left) and H-H (right). The incident angle is $\theta^i=0^\circ$.

The second example is taken from [8]. It is made of two sections of circular cylinders, one PEC and one dielectric. The side view of the structure as well as the dimension parameters are shown in Fig. 5. The relative permittivity of the dielectric is 2.6, and the incident plane wave frequency is 3.0 GHz.

For the "SIE+VIE" modeling, SIE is applied to the material surface (no part of material is modeled with VIE for this example). The number of unknowns is N=6,672, CPU time is T = 35.8 s per incident angle, and total memory used is M = 113 MB. For "VIE ONLY" modeling, the run time parameters are N=17,280, T=92.05s, and M = 1,171 MB. It is seen that the "SIE+VIE" approach uses almost three times less number of unknowns compared to the "VIE ONLY" approach. The latter also uses more CPU time per incident angle (this is an example for which "VIE ONLY" approach is not efficient to apply). The computed mono-static RCSs by both approaches are shown in Fig. 6, from which, we can see good agreement between the two results.

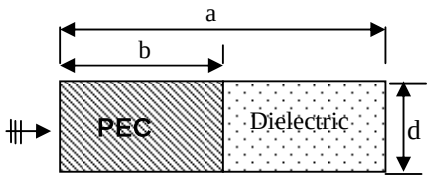

Fig. 5. The side view of a composite PEC and dielectric cylindrical scatterer of circular cross section (a = 15.24 cm, b = 10.16 cm, d = 7.62 cm). The incident $\theta^i=0$ is on PEC side of the axis (shown by the arrow in the figure).

The next example is a composite triangular plate that is made by two material regions and a PEC surface, as shown in Fig. 7. Material-2 (with permittivity ε_2) is considered as embedded within material-1 (with permittivity ε_1). For "SIE+VIE" modeling, N=17,959, CPU time is T = 76.7 per incident angle, total memory is 355 MB, and average iteration number per angle is $\bar{N}_{\text{itr}}$ = 41.9 (it equals the total iteration number for all incident angles divided by number of incident angles). For "VIE ONLY" modeling, the runtime parameters are N = 24,219, T = 8.6s, M = 427 MB, and $\bar{N}_{\text{itr}}$ =5.66. The numbers of iterations explain why the CPU time for the "SIE+VIE" approach is more than that of "VIE ONLY" approach. Because the overall thickness of the structure is thin ($0.4\lambda_0$), the "VIE ONLY" approach is more efficient to apply for this example. The two results are given in Fig. 8 and they agree well to each other.

In the last example, we consider a composite cylinder of finite length as shown in Fig. 9. The cross section of this cylinder is an ogive, and the two edges (parallel to z-axis) are coated by materials of $\varepsilon_{r1}=\varepsilon_{r2}=2.5+0.5i$. The width of the coating with ε_1 (in the +x side) is 0.236m, and that with ε_2 (in –x side) is 0.115m. For "SIE+VIE" modeling, N = 16,052, T = 110 s, and M = 196 MB. For "VIE ONLY" modeling, the runtime parameters are N = 19,446, T = 43.7 s, and M = 172.8 MB. The calculated RCSs at 1.0 GHz incidence are shown in Fig. 10.

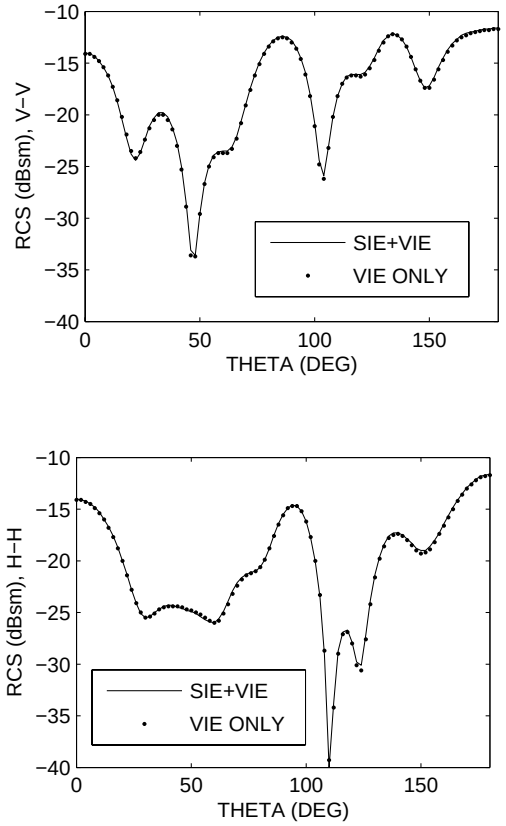

Fig. 6. Mono-static RCSs of a composite cylindrical scatterer for V-V polarization (left) and H-H polarization (the description of the cylinder is in Fig. 5).

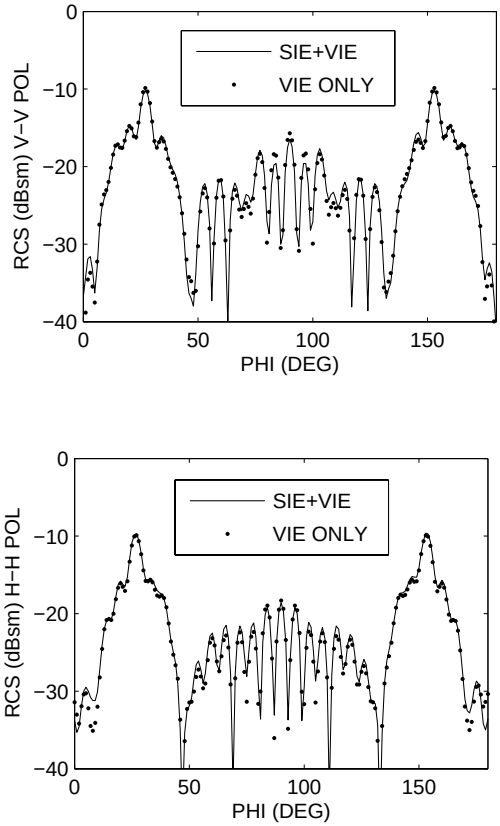

Fig. 8. The mono-static RCSs of the composite plate of Fig. 7. The incident wave frequency is 3.0 GHz, and the results are for the $\theta^i = 90^\circ$ plane.

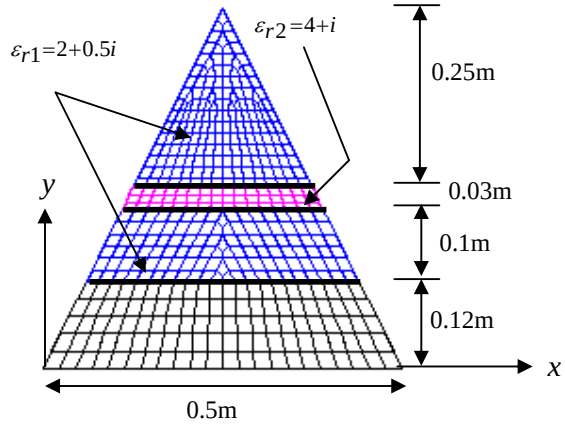

Fig. 7. The top view of a composite triangular plate that is made by 3 parts, a conducting part (bottom), and two dielectric regions. The middle dielectric (with ε_{r2}) is considered as embedded within the material of ε_{r1}. The thickness of the plate is 0.04 m.

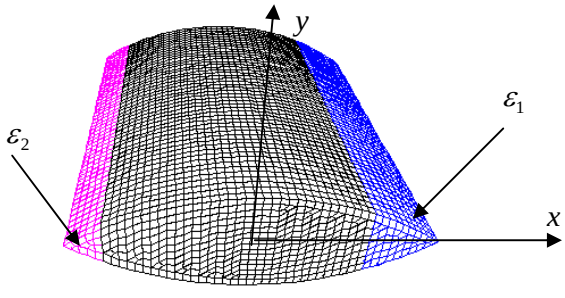

Fig. 9. A composite finite-length cylinder of ogive cross section is made of two dielectric materials and a PEC body. The sizes in x, y, and z-directions are 1.4 m, 0.36 m, and 1.44 m, respectively.

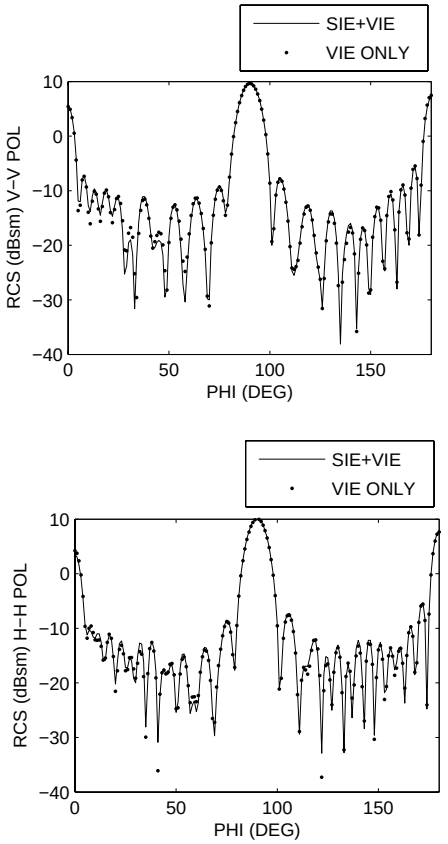

Fig. 10. The calculated RCSs for the ogive cylinder of Fig. 9 for V-V polarization (left) and H-H polarizations (right).

IV. CONCLUSIONS

In this work, we implemented a hybrid "SIE+VIE" formulation for computing the scattering by composite scattereres that made of larger conducting and dielectric materials. This formulation takes the advantage of SIE for large homogeneous material regions, and that of VIE for small and thin material regions. It is applicable to scattering problems with multiple material regions of different sizes and shapes. When a material region is electrically large, the MLFMA is applied to accelerate the matrix-vector multiplication in the iterative solution process. Numerical examples are presented that verified the solution accuracy of the hybrid formulation, and demonstrated its ability in solving large and complex scattering problems. This work applied one type of fast solver only (the MLFMA) which is not the best choice for all domains or for all problem configurations. In fact, based on domain shape and size, it is possible to use different types of fast solvers for different domains to achieve optimum performance. This remains to be a future implementation.

REFERENCES

[1] K. Umashankar, A. Taflove, and S. M. Rao, "Electromagnetic scattering by arbitrary shaped three-dimensional homogeneous lossy dielectric objects," *IEEE Trans. Antennas Propagat*., vol.34, no. 6, pp. 758-766, June 1986.

[2] R. F. Harrington, "boundary integral formulations for homogeneous material bodies," *J. Electromag. Waves Appl*., vol. 3, no. 1, pp. 1-15, 1989.

[3] S. M. Rao, D. R. Wilton, and A. W. Glisson, "Electromagnetic scattering by surfaces of arbitrary shape," *IEEE Trans. Antennas Propagat*., vol. 30, no. 3, pp. 409-418, May 1982.

[4] T. K. Wu and L. L. Tsai, "Scattering from arbitrarily-shape lossy dielectric bodies of revolution," *Radio Sci*., vol. 12, no.5, pp. 709-718, 1977.

[5] P. Yla-Oijala, M. Taskinen, and J. Sarvas, "Surface integral equation for general composite metallic and dielectric structures with junctions," *Progress In Electromagnetics Research*, PIER-52, pp. 81-108, 2005.

[6] E. Arvas, A. Rahhal-Arabo, A. Sadigh, and S. M. Rao, "Scattering from multiple conducting and dielectric bodies of arbitrary shape," *IEEE Trans. Antennas and Propagat*., vol. 33, no. 2, pp. 29-36, April 1991.

[7] P. L. Huddleston, N. Medgyesi-Mitschang, and J. M. Putnam, "Combined field integral equation formulation for scattering by dielectrically coated conducting bodies," *IEEE Trans. on Antennas and Propagat*., vol. 34, no. 4, pp. 510-520, April 1986.

[8] L. N. Medgyesi-Mitschang and J. M. Putnam, "Electromagnetic Scattering from Axially Inhomogeneous Bodies of Revolution," *IEEE Trans. Antennas Propagat*., vol. 32, no. 8, pp. 797-806, Aug. 1984.

[9] K. Donepudi, J. M. Jin, and W. C. Chew, "A higher order multilevel fast multiple algorithm for scattering from mixed conducting/dielectric bodies," *IEEE Trans. Antennas and Propagat*., vol. 51, no. 10, pp. 2814-2821, Oct. 2003.

[10] S. M. Rao and D. R. Wilton, "E-field, H-field, and combined field solution for arbitrarily shaped three-dimensional dielectric bodies," *Electromagnetics*, vol. 10, pp. 407-421, 1990.

[11] J. P. Kottmann and O. J. Martin, "Accurate solution of volume integral equation for high-permittivity scatterers," *IEEE Trans. on Antennas and Propagat*., vol. 48, no. 11, pp. 1719-1726, Nov. 2000.

[12] C. C. Lu and W. C. Chew, "A coupled surface-volume integral equation approach for the calculation of electromagnetic scattering from composite metallic and material targets," *IEEE Trans. Antennas Propagat*., vol. 48, no. 12, pp. 1866-1868, Dec. 2000.

[13] D. E. Livesay and K. M. Chen, "Electromagnetic fields induced inside arbitrary shaped biological

bodies," *IEEE Trans. Micro. Theory Tech.*, vol. 22, no. 12, pp. 1273-1280, Dec. 1974.

[14] D. H. Schaubert, D. R. Wilton, and A. W. Glisson, "A tetrahedral modeling method for electromagnetic scattering by arbitrary shaped inhomogeneous dielectric bodies," *IEEE Trans. Antennas Propagat.*, vol. 32, no. 1, pp. 77-85, Jan. 1984.

[15] S. Gedney and C. C. Lu**,** "High-order solution for the electromagnetic scattering by inhomogeneous dielectric bodies," *Radio Sci.*, vol. 38, no. 1, pp. 15-1 to 15-8, 2003.

[16] C. Yu and C. C. Lu, "Analysis of Finite and Curved Frequency Selective Surfaces Using the Hybrid Volume-Surface Integral Equation Approach," *Micro. Opt. Tech. Lett*., vol. 45, no. 2, pp. 107-112, April 2005.

[17] M. I. Sancer, K. Sertel, J. L. Volakis, and P. V. Alstine, "On volume integral equations", *IEEE Trans. Antennas Propagat.*, vol. 54, no. 5, pp. 1488-1495, May. 2006.

[18] C. C. Lu and C. Luo, "Comparison of iteration convergences of SIE and VSIE for solving electromagnetic scattering problems for coated objects", *Radio Sci.*, vol. 38, no. 2, pp. 11-1 to 11-9, 2003.

[19] R. Coifman, V. Rokhlin, and S. Wandzura, "The Fast Multipole Method for the Wave Equation: A Pedestrian Prescription," *IEEE Antennas and Propagat. Magazine*, vol. 35, no. 3, June 1993.

[20] J. M. Song and W. C. Chew, "Multlevel Fast-Multipole Algorithm for Solving Combined Field Integral Equations of Electromagnetic Scattering," *Microwave Opt. Tech. Lett.*, vol. 10, no. 1, Sep.1995.

Cai-Cheng Lu received the Ph.D. degree from University of Illinois at Urbana Champaign in 1995. He is now an associate professor in the Department of Electrical and Computer Engineering at the University of Kentucky. Priori to join University of Kentucky, He was with Science Application International, Inc., where he worked on a number of new features for the XPATCH code. His research interests are in wave scattering, microwave circuit simulation, and antenna modeling. He is especially experienced in fast algorithms for computational electromagnetics and is one of the authors for a CEM code FISC. He is a recipient of the 2000 Yong Investigator Award from the Office of Naval Research, and a CAREER Award from the National Science Foundation. Dr. Lu is a senior member of IEEE.

Chong Luo was born in Sichuan, China, in 1972. He received B.S. degree, in Electrical Engineering from Beijing University of Aeronautics and Astronautics, Beijing, China, in 1994, the M.S. and Ph.D. degrees in Electrical Engineering from University of Kentucky, Lexington, in May 2002 and December 2006. He is currently with the Electrical Engineering Department, University of Kentucky. His primary research interest is in computational electromagnetics. Dr. Luo is a member of IEEE.